Synthesis and Characterization of Methyltrioxorhenium(VII) Immobilized in Bipyridyl-Functionalized Mesoporous Silica

Carla D. Nunes,[a] Martyn Pillinger,[a] Anabela A. Valente,[a] Isabel S. Gonçalves,*[a] João Rocha,[a] Paula Ferreira,[b] and Fritz E. Kühn*[b]

Keywords: Rhenium / Supported catalysts / Mesoporous materials / Lewis base adducts

Methyltrioxorhenium(VII) (MTO) has been immobilized in the mesoporous silica MCM-41 functionalized with pendant bipyridyl (bpy) groups of the type 4-[(–O)$_3$Si(CH$_2$)$_4$]-4′-CH$_3$-2,2′-bipyridine. Powder X-ray diffraction and N_2 adsorption-desorption studies confirm that the regular hexagonal symmetry of the host is retained during the grafting reaction and that the channels remain accessible. Solid-state magic angle spinning NMR spectroscopy (^{29}Si, ^{13}C) was also used to monitor the coupling reactions. The formation of a tethered Lewis base adduct of the type CH$_3$ReO$_3$·bpy is confirmed by IR, Raman, and X-ray absorption fine structure (XAFS) spectroscopy. The XAFS results do, however, indicate that not all rhenium ions are present in this form, and this agrees with elemental analysis which gives an Re/N ratio of 1:1.1 (0.55 mmol Re g^{-1}). It is likely that the excess rhenium atoms are present as uncoordinated MTO molecules assembled in the MCM channels. The model complexes (4-alkyl-4′-methyl-2,2′-bipyridine)(methyl)trioxorhenium (alkyl = methyl, *n*-butyl) were also prepared and characterized.

Introduction

Methyltrioxorhenium(VII) (MTO) has excellent catalytic properties in numerous oxy functionalizations,[1] some examples being the oxidation of olefins,[2] alcohols,[3] arenes,[4] and carbonylmetal compounds.[5] The epoxidation of olefins has received particular attention, using MTO to activate H_2O_2. Due to the Lewis acidity of the rhenium center, a major limitation of this system is the opening of the epoxide ring, leading to the formation of diols in the presence of water.[1,6] It was soon found, however, that amine additives, such as pyridine,[7] pyrazole,[8] and 3-cyanopyridine,[9] enhance the efficiency and selectivity of MTO-catalyzed oxidations. The aromatic N-base ligands work by coordinating to the metal center, thereby reducing the Lewis acidity of the catalyst and additionally accelerating the catalytic reactions. MTO forms trigonal-bipyramidal adducts with pyridines and related bases,[10a] and distorted octahedral adducts with bidentate Lewis bases, e.g. 4,4′-dimethyl-2,2′-bipyridine, 1,10-phenanthroline, and 2,2′-bipyrimidine.[10b] In the presence of H_2O_2 these complexes form very active and highly selective epoxidation catalysts.

Alternative strategies to improve MTO-catalyzed oxidations have involved host-guest inclusion chemistry. It was found that a urea/hydrogen peroxide complex is a very effective oxidant in heterogeneous olefin epoxidations and silane oxidations catalyzed by MTO.[11] With NaY-zeolite as host for these reactions also resulted in high yields and excellent product selectivities.[12] MTO has also been supported on silica functionalized with polyether tethers.[13] In the absence of an organic solvent, this catalytic assembly catalyzed the epoxidation of alkenes with 30% H_2O_2 with high selectivity compared to the ring-opened products observed in homogeneous media. In another example, MTO was heterogenized inside the porous system of a hybrid silica matrix by the sol-gel method using 4-[3-(triethoxysilyl)-propylamino]pyridine hydrochloride as a hydrolyzable ligand.[14] A supported catalyst of this type could, in principle, combine the advantages of a Lewis base adduct of MTO with the well-known benefits of a heterogeneous host-guest catalyst system.

Recently, we devised a stepwise procedure for the functionalization of the ordered mesoporous silica MCM-41 with pendant 4-alkyl-4′-methyl-2,2′-bipyridine groups.[15] Elemental analysis, powder X-ray diffraction (XRD), N_2 adsorption-desorption, solid-state magic angle spinning (MAS) NMR (^{13}C, ^{29}Si) and IR spectroscopy were used to monitor the different coupling reactions. The ligand−silica was subsequently examined as a support for the hetero-

[a] Department of Chemistry, University of Aveiro, Campus de Santiago,
3810-193 Aveiro, Portugal
Fax: (internat) + 351-234/370084
E-mail: igoncalves@dq.ua.pt
[b] Anorganisch-chemisches Institut der Technischen Universität München,
Lichtenbergstraße 4, 85747 Garching bei München, Germany
Fax: (internat) + 49-89/28913473
E-mail: fritz.kuehn@ch.tum.de

genization of the dioxomolybdenum(VI) complex $MoO_2Cl_2(THF)_2$. Instead of forming surface-bound monomeric complexes of the type $MoO_2Cl_2(bpy)$, weakly bound oxo-bridged dimers were formed with a metal−metal separation of 3.28 Å. In the present work, MTO is used as the oxometal species rather than the fragment MoO_2Cl_2, with the intention of forming surface-bound Lewis base adducts of the type **1**. The known MTO adduct **2**, containing the ligand 4,4′-dimethyl-2,2′-bipyridine, and also the novel complex **3**, containing the asymmetrical bipyridine ligand 4-(*n*-butyl)-4′-methyl-2,2′-bipyridine, have been prepared as model compounds. The hybrid material has been characterized by Raman spectroscopy and Re L-edge X-ray absorption fine structure (XAFS) spectroscopy, in addition to the techniques mentioned above.

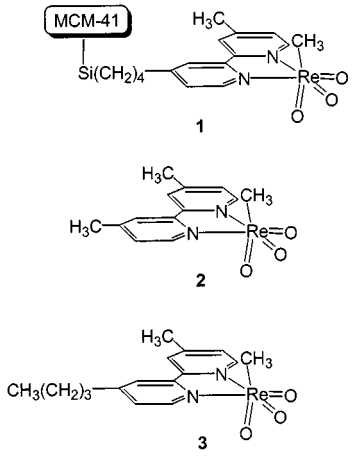

Results and Discussion

The preparation and characterization of MCM-41 functionalized with bipyridyl groups has been described in a previous paper.[15] In the first step, the pristine calcined hexagonally ordered mesoporous host (d_{100} = 36.3 Å, a = 41.9 Å) is covalently grafted with (3-chloropropyl)trimethoxysilane. The second step comprises substitution of about 21% of pendant chloro groups by the anion [4-CH_2-4′-CH_3-2,2′-bipyridine]$^-$ to give a material containing about 0.3 mmol bipyridyl groups per gram, designated as MCM-41-bpy. Powder XRD and N_2 adsorption-desorption analysis demonstrate that the textural characteristics of the support are preserved during the grafting experiments and that the channels remain accessible (BET specific surface area 720 $m^2\ g^{-1}$, total pore volume 0.37 $cm^3\ g^{-1}$).

The heterogenization of MTO was carried out by treating the ligand−silica MCM-41-bpy (0.5 g) with a dichloromethane solution of MTO (0.046 M, 0.92 mmol) at room temperature. The resulting material, designated as MCM-41-bpy/MTO, was recovered by filtration and washed repeatedly with dichloromethane. Drying the product under vacuum at room temperature did not liberate (sublime) MTO from the MCM channels (pure MTO sublimes at 25 °C when using an oil-pump vacuum). The material is moderately air- and light-sensitive. Elemental analysis indicated a metal loading of 10.24 mass-% Re (0.55 mmol g^{-1}), giving an Re/N molar ratio of 1:1.1. If it is assumed that all Re is present as MTO, and knowing the specific total pore volume before and after introduction of MTO (see below), the volume occupied by MTO molecules in MCM-41-bpy/MTO is calculated to be 0.04 $cm^3\ g^{-1}$. It follows that the mass of MTO molecules per unit volume occupied is 3.5 g cm^{-3} [= 0.1024×(249.2/186.2)/0.04]. This value is similar to the density of bulk MTO (4.1 g cm^{-3}).

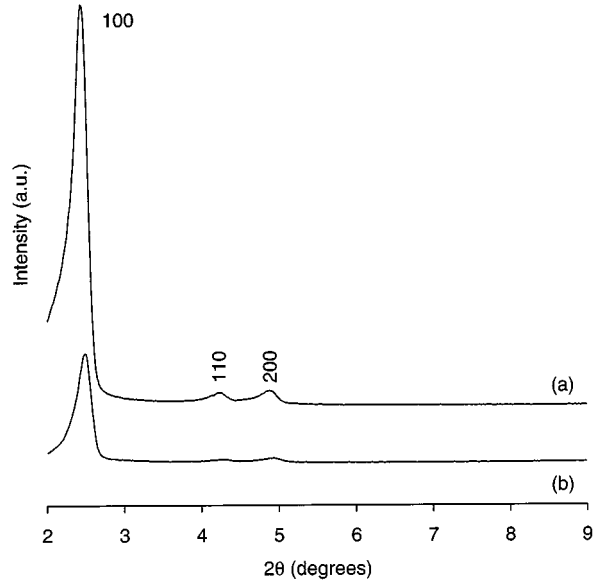

Figure 1. Powder XRD patterns of (a) MCM-41-bpy and (b) MCM-41-bpy/MTO

Figure 1 shows the powder XRD patterns of MCM-41-bpy and MCM-41-bpy/MTO. Three reflections are observed in the range 2θ = 2−8° for MCM-41-bpy, indexed assuming a hexagonal cell as (100), (110), and (200). The d value of the (100) reflection is 36.0 Å leading to a lattice constant of a = 41.6 Å. Three reflections are also observed for MCM-41-bpy/MTO, indicating retention of the long-range hexagonal symmetry. There is a slight contraction of the unit cell (d_{100} = 35.4 Å, a = 40.9 Å) and the intensities of the three reflections are considerably reduced compared to the starting ligand−silica. This is not interpreted as a severe loss of crystallinity. Instead, it is likely that there is a reduction in the X-ray scattering contrast between the silica wall and pore-filling material.[16] A similar phenomenon was observed for treatment of MCM-41-bpy with the complex $MoO_2Cl_2(THF)_2$,[15] and MCM-41 grafted with multiply bonded dimolybdenum complexes.[17]

Figure 2 shows the low-temperature N_2 adsorption-desorption isotherm for MCM-41-bpy/MTO. The corresponding isotherms for the pristine calcined MCM-41 host and the ligand−silica MCM-41-bpy are also shown for comparison. Each isotherm can be classified as type IV as defined by IUPAC,[18] characteristic of mesoporous solids (having pore widths between 2 and 50 nm). The isotherms show no evidence of hysteresis loops resulting from capillary condensation/evaporation, which has been attributed

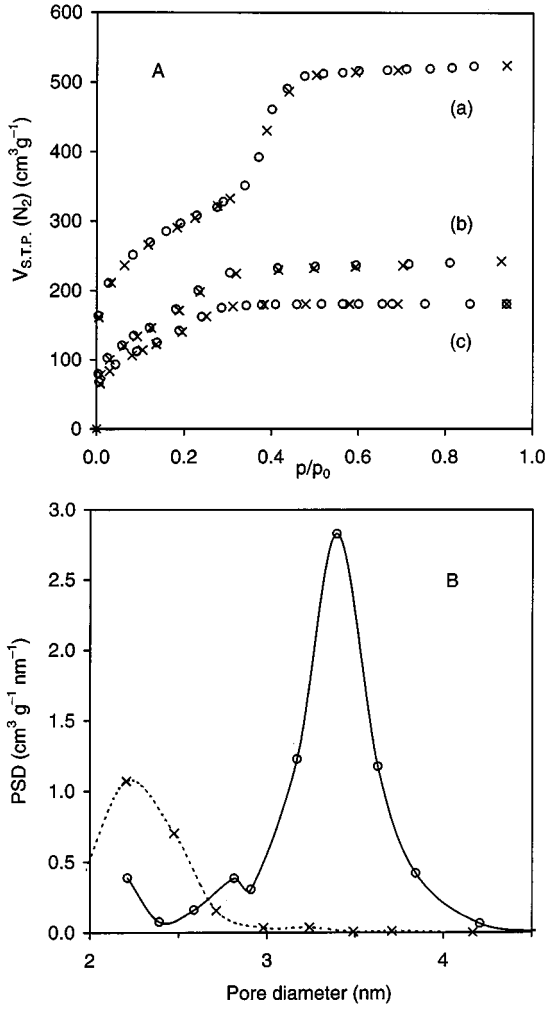

Figure 2. A: N_2 adsorption (×) and desorption (O) isotherms at 77 K of (a) pristine MCM-41, (b) MCM-41-bpy and (c) MCM-41-bpy/MTO; B: pore-size distribution profiles for pristine MCM-41 (——) and MCM-41-bpy/MTO (···)

to the instability of the liquid nitrogen meniscus.[18] Each of the modifications carried out to produce the two derivatized samples MCM-41-bpy and MCM-41-bpy/MTO leads to a decrease in the N_2 uptake at any given p/p_0, and both the BET specific surface area and pore volume decrease (Table 1). In the case of MCM-41, a pronounced step is observed between relative pressures of 0.32 and 0.42, arising from the condensation of nitrogen inside the primary mesopores. The sharpness of this step reflects the uniform pore size. A comparison of the pore size distribution (PSD) curves for MCM-41 and MCM-41-bpy/MTO reveals that the position of the maximum decreases from 34 to 23 Å (Figure 2). The decrease in the intensity of the maximum, together with an increase in the width at half height, indicates an increase in pore heterogeneity.

The material MCM-41-bpy/MTO was further characterized by thermogravimetric analysis (TGA), IR, Raman, MAS NMR, and XAFS spectroscopy. In order to assist the interpretation of these results, the known adduct **2** and the novel derivative **3** were prepared as model compounds. These complexes are readily obtained as yellow solids by

Table 1. Texture parameters of MCM-41 samples from N_2 isotherms at 77 K

Sample	S_{BET} [$m^2\ g^{-1}$]	ΔS_{BET} (%)[a]	V_P [$cm^3\ g^{-1}$]	ΔV_P (%)[b]
MCM-41	1029	–	0.81	–
MCM-41-bpy	718	−30	0.37	−54
MCM-41-bpy/MTO	574	−44	0.28	−66

[a] Variation of surface area in relation to parent MCM-41. [b] Variation of total pore volume in relation to parent MCM-41.

the reaction of MTO with 1 equiv. of bidentate N,N-ligand in tetrahydrofuran (THF) at room temperature (Scheme 1). Spectroscopic data (IR and ^1H NMR) for **2** are in agreement with that reported.[10b] The ^1H and ^{13}C NMR chemical shifts for the Re−CH_3 groups in **2** are located at δ = 1.20 and 25.9, respectively.[10b] The shifts in these resonances compared to those of uncoordinated MTO [δ(^{13}C) = 19.03; δ(^1H) = 2.67] are a consequence of electron donation to the Lewis-acidic metal center. In fact it has been shown that the weaker the donor ability of the Lewis base, the closer, in general, are the observed δ(^1H) and δ(^{13}C) values to those of uncoordinated MTO.[10] In the case of **3**, δ(^1H) and δ(^{13}C) of Re−CH_3 are located at δ = 1.09 and 26.0, respectively, and therefore the ligand in **3** can be considered as being a slightly stronger donor than that in **2**.

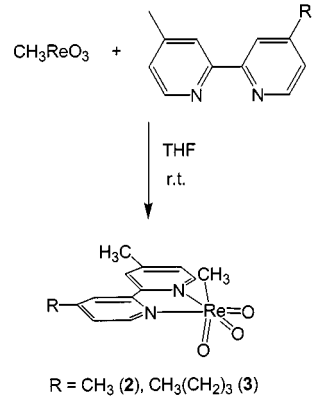

Scheme 1

TGA of MCM-41-bpy/MTO shows that the material decomposes in three steps up to 750 °C. It is stable under nitrogen up to about 50 °C, but then undergoes an abrupt mass loss, losing 6.0% up to 100 °C and a further 2.3% up to 200 °C. It is assumed that this is due to decomposition/sublimation of encapsulated MTO (MTO sublimes below 100 °C under TG conditions[19]). Further heating gives a residual mass of 81% at 750 °C. For comparison, the adduct CH_3ReO_3(4,4′-dimethyl-2,2′-bipyridine) (**2**) is stable under nitrogen up to 110 °C, then undergoes an abrupt mass loss of 24% up to 180 °C. This must correspond to rupture of the Re−N bond and sublimation of the now uncoordinated MTO. At 750 °C 42% remains as residual mass.

The IR spectrum of MCM-41-bpy/MTO contains one split band at 917 cm^{-1} (922 and 912 cm^{-1}) that is not observed in the spectrum of the ligand−silica MCM-41-bpy. This is attributed to an asymmetric Re=O stretching vibration. An associated symmetric stretching vibration should be present at higher frequency but is probably obscured by a broad band at 961 cm^{-1} arising from the silica host. The Raman spectrum shows more clearly the bands corresponding to the symmetric and asymmetric Re=O stretching vibrations (940 and 918 cm^{-1}, Figure 3). The model compound **3** displays very similar IR (940 and 919 cm^{-1}) and Raman (937 and 916 cm^{-1}) absorptions. From the IR data for **3** the force constant of the Re=O vibration can be calculated[20] to be 7.41 mdyn $Å^{-1}$. The corresponding bands for bulk MTO appear at 999 cm^{-1} (symmetric) and 957 cm^{-1} (asymmetric), yielding a force constant of 8.46 mdyn $Å^{-1}$.[10b] The decrease in the force constant indicates a weakening of the Re=O bonds, caused by electron donation from the coordinated bipyridyl groups to the Re^{VII} center.[10,21]

Further evidence for the formation of surface-bound adducts of the type $CH_3ReO_3(N-N)$ in MCM-41-bpy/MTO comes from the Raman bands of the tethered bipyridine groups. The precursor ligand−silica MCM-41-bpy displays bands at 1607 and 1559 cm^{-1} due to pyridyl ring stretching vibrations, and a band at 997 cm^{-1} due to an in-plane ring C−H deformation vibration (Figure 3). The corresponding ligand 4-(*n*-butyl)-4′-methyl-2,2′-bipyridine displays three identical bands. In complex **3** these bands shift to 1615, 1555 and 1030 cm^{-1}. Very similar results are obtained for the functionalized material MCM-41-bpy/MTO (bands at 1611, 1555 and 1031 cm^{-1}). The Raman spectrum of this material also contains a weak band at 997 cm^{-1}. This could be due to the ring C−H deformation vibration of uncoordinated bipyridyl groups, or alternatively to the Re=O symmetric stretching vibration of uncoordinated MTO molecules aggregated in the MCM channels. The Raman spectra of the complexes **2** and **3** contain a weak band at 555 cm^{-1} due to the Re−C stretching vibration (cf. 575 cm^{-1} for bulk MTO), and also a strong band at about 475 cm^{-1} that does not appear in the spectra of either the corresponding free ligand or bulk MTO. This latter band may be due to a C−Re=O deformation vibration.[22] While a band for the Re−C stretching vibration is not observed in the Raman spectrum of the material MCM-41-bpy/MTO, a band is clearly seen at 474 cm^{-1} that does not appear in the spectrum of MCM-41-bpy.

The ^{29}Si MAS and CP MAS NMR spectra of MCM-41-bpy/MTO are similar to those of the precursor MCM-41-bpy (Figure 4).[15] Two broad overlapping peaks at $\delta = -109.8$ and -102.0 are assigned to Q^4 and Q^3 units, respectively, of the silica framework, where $Q^n = Si(OSi)_n(OH)_{4-n}$. Two signals are also observed at $\delta = -58.7$ and -66.7, assigned to T^2 and T^3 organosilica species, respectively [$T^m = RSi(OSi)_m(OMe)_{3-m}$]. The ^{13}C CP MAS NMR spectrum of MCM-41-bpy/MTO is also largely unchanged compared to that of MCM-41-bpy (Figure 5).

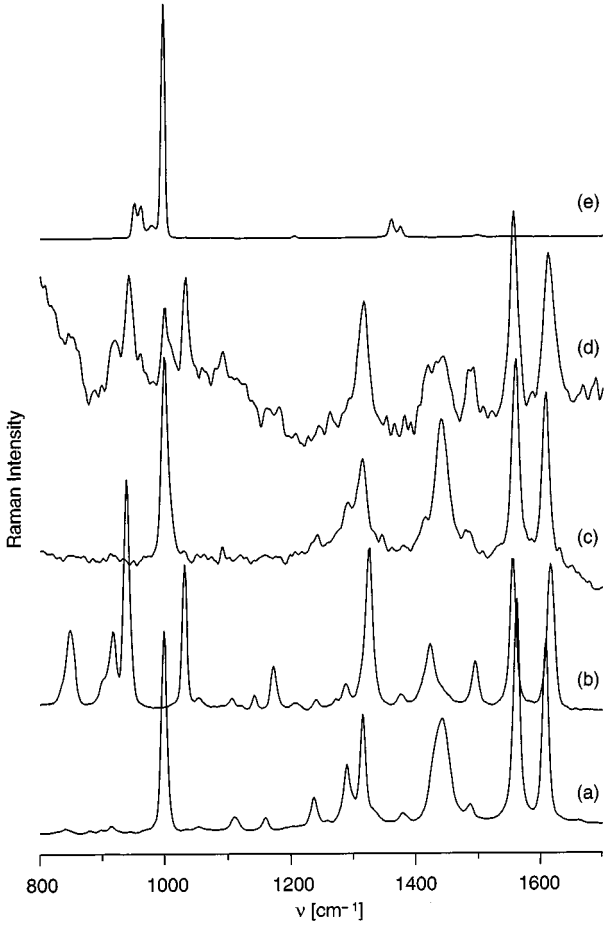

Figure 3. Raman spectra of (a) 4-(*n*-butyl)-4′-methyl-2,2′-bipyridine, (b) [4-(*n*-butyl)-4′-methyl-2,2′-bipyridine](methyl)trioxorhenium (**3**), (c) MCM-41-bpy, (d) MCM-41-bpy/MTO and (e) CH_3ReO_3

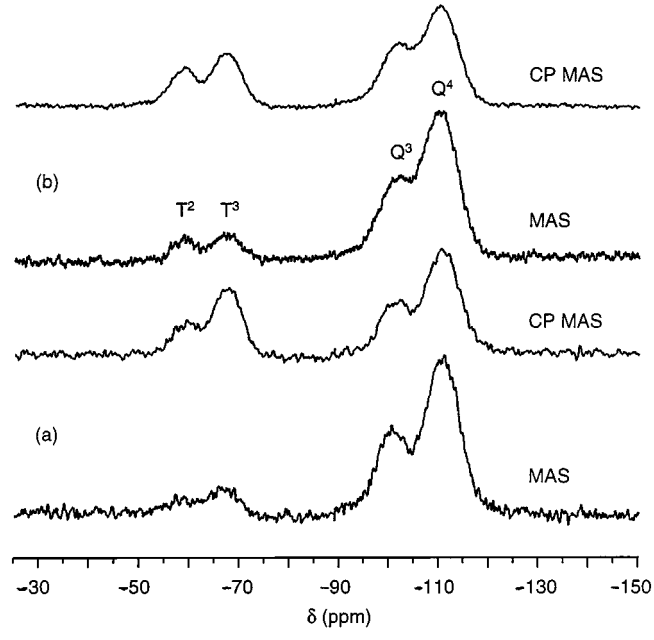

Figure 4. ^{29}Si MAS and CP MAS NMR spectra of (a) MCM-41-bpy and (b) MCM-41-bpy/MTO

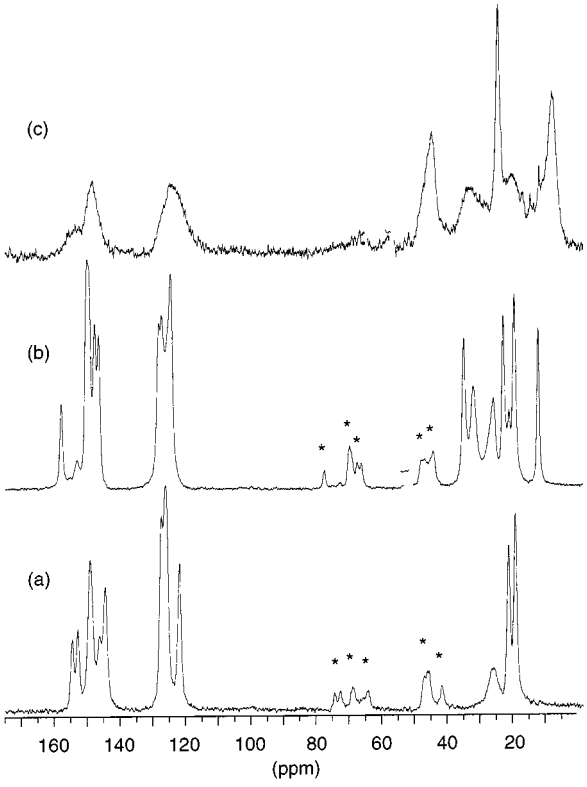

Figure 5. ^{13}C CP MAS NMR spectra of (a) (4,4′-dimethyl-2,2′-bipyridine)(methyl)trioxorhenium (**2**), (b) [4-(*n*-butyl)-4′-methyl-2,2′-bipyridine](methyl)trioxorhenium (**3**), and (c) MCM-41-bpy/MTO; asterisks denote spinning sidebands

Assignment of these spectra was supported by measuring the solution spectra of the ligand 4-(*n*-butyl)-4′-methyl-2,2′-bipyridine, and the MTO adduct of this ligand (**3**). Solid-state MAS NMR spectra were also recorded for **2** and **3** (Figure 5). In the ^{13}C CP MAS NMR spectrum of MCM-41-bpy/MTO, two broad peaks at δ = 149.3 and 125.7, and a shoulder at δ = 155.0, are assigned to the pyridyl ring carbon atoms. The other signals in the spectrum are attributed as follows: δ = 46.1 [Si(O*Me*)$_n$CH$_2$R and −*C*H$_2$Cl], 35.0 (−*C*H$_2$*C*H$_2$−bpy), 26.0 [Re−CH$_3$ and Si(OMe)$_n$CH$_2$*C*H$_2$−], 21.8 (*C*H$_3$−bpy), 9.6 [Si(OMe)$_n$-*C*H$_2$R]. Treatment of MCM-41-bpy with MTO produces only one measurable change in the ^{13}C NMR spectrum: the signal at δ = 123.3 shifts to δ = 125.7. A similar shift difference is observed for the corresponding resonances of the ligand 4-(*n*-butyl)-4′-methyl-2,2′-bipyridine and the MTO adduct of this ligand (**3**).

XAFS measurements at the Re L_I and L_{III} absorption edges were carried out at low temperature (20 K) for the Lewis base adduct **2** and MCM-41-bpy/MTO. The Re L_I X-ray absorption near edge structure (XANES) spectrum of **2** contains a weak pre-edge peak, caused by a 2s → 5d(Re) + 2p(O) electron transition (Figure 6).[23] With respect to the rhenium coordination, the intensity of this peak is usually strongest for systems with non-inversion symmetry, such as tetrahedral coordination. MTO, for example, exhibits an intense sharp pre-edge peak.[24] Any distortion of the regular tetrahedral symmetry leads to a decrease in the peak intensity. The XANES spectrum of **2** is therefore consistent with the expected rhenium coordination, i.e. distorted octahedral geometry. It is obvious that the XANES spectrum of MCM-41-bpy/MTO is quite different from that of **2**, in that the pre-edge peak is stronger and there are differences in the oscillations towards higher energy (Figure 6). In fact, the spectrum of MCM-41-bpy/MTO comes close to that reported for bulk MTO.[24]

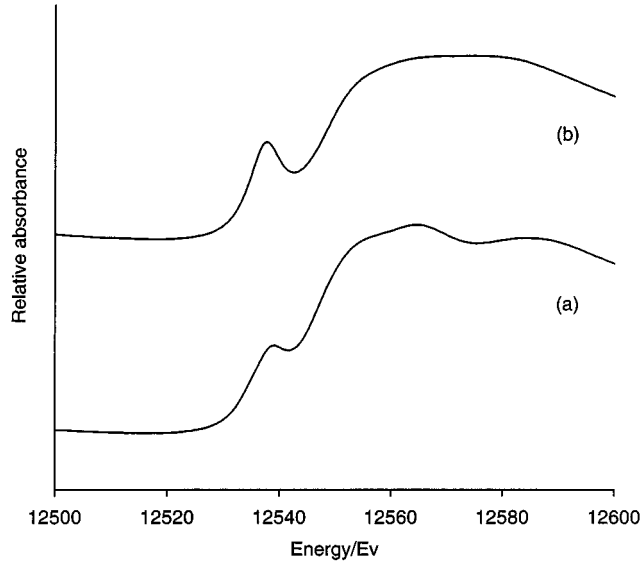

Figure 6. Re L_I-edge XANES spectra of (a) (4,4′-dimethyl-2,2′-bipyridine)(methyl)trioxorhenium (**2**), and (b) MCM-41-bpy/MTO

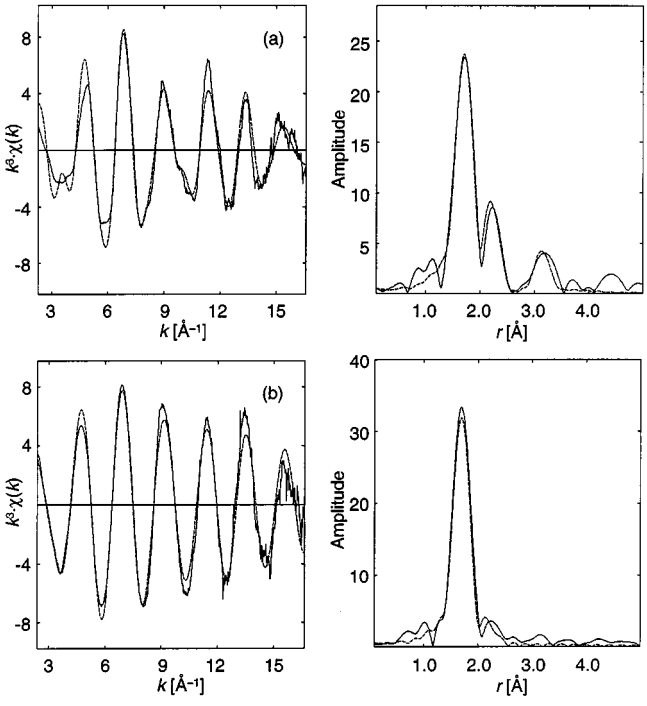

Figure 7. Re L_{III}-edge XAFS and Fourier transforms for (a) (4,4′-dimethyl-2,2′-bipyridine)(methyl)trioxorhenium (**2**), and (b) MCM-41-bpy/MTO; the solid line represents the experimental data and the dashed line shows the best fit using parameters given in Table 2

Table 2. Re L_{III}-edge XAFS-derived structural parameters for (4,4′-dimethyl-2,2′-bipyridine)(methyl)trioxorhenium (**2**) and MCM-41-bpy/MTO

Compound	Atom	CN[a]	r [Å]	$2\sigma^2$ [Å^2][b]	E_f [eV][c]	R (%)[d]
2[e]	O	3.0(1)	1.741(2)	0.0048(3)	−13.8(5)	27.2
	N	2.5(2)	2.246(5)	0.0052(8)		
	C	4.0(6)	3.192(11)	0.0078(19)		
MCM-41-bpy/MTO	O	3.3(1)	1.729(1)	0.0027(2)	−11.2(5)	19.0
	N	1.3(3)	2.216(11)	0.0091(24)		

[a] CN = Coordination number. Values in parentheses are statistical errors generated in EXCURVE. The true errors in coordination numbers are likely to be of the order of 20%; those for the interatomic distances ca. 1.5%.[25] [b] Debye−Waller factor; σ = root-mean-square internuclear separation. [c] E_f = edge position (Fermi energy), relative to calculated vacuum zero. [d] $R = (\int[\Sigma^{theory} - \Sigma^{exp.}]k^3 dk / [\Sigma^{exp.}]k^3 dk) \times 100\%$. [e] Compound **2** has been examined by single-crystal X-ray crystallography,[10b] but bond lengths and bond angles could not be determined reliably because the structure is disordered with respect to the position of the metal center.

Analysis of the Re L_{III} XAFS spectrum of **2** allowed three shells for O, N and C neighbors to be determined, in order of increasing distance from the absorbing atom (Figure 7, Table 2). The Re−O bond length of 1.74 Å is typical of all known (oxo)Re^{VII} complexes containing an Re=O double bond.[1f] Bidentate coordination of the bipyridyl ligand is confirmed by the presence of the other two shells for N (2.25 Å) and C (3.19 Å). The Re−N bond length is comparatively long, indicating a weak N→Re bonding interaction. Identical Re−N bond lengths were determined by single-crystal X-ray crystallography for the adducts $XReO_3$[4,4′-bis(*tert*-butyl)-2,2′-bipyridine] (X = Cl, Br).[26] The Re···N shell almost certainly includes a component for the carbon shell corresponding to Re−C, expected at about 2.1 Å. The similarity of the two elements as back-scatterers, together with the close proximity of the two shells, means that only one shell can be fitted. The Re L_{III} XAFS of MCM-41-bpy/MTO was initially fitted by a model comprising one shell of oxygen atoms. Both the refined distance (1.74 Å) and coordination number (3.3) are consistent with the presence of trioxorhenium species. Addition of a second shell for nitrogen atoms at 2.22 Å (coordination number = 1.3) reduced the R factor from 23.2 to 19.0% (Table 2, Figure 7). This shell was significant at the 99% level according to the statistical test of Joyner et al.[27] There was no evidence for a well-defined Re···Re outer coordination shell.

Conclusions

MCM-41 functionalized with bipyridyl groups has been successfully used as a support for the immobilization of methyltrioxorhenium(VII). Powder XRD and N_2 adsorption-desorption studies confirm that the regular hexagonal symmetry of the mesoporous host is retained during the grafting reaction and that the channels remain accessible. The formation of a tethered Lewis base adduct of the type CH_3ReO_3(bpy) is substantiated by IR, Raman, and XAFS spectroscopy. The latter technique does, however, indicate that not all rhenium atoms are present in this form and this is consistent with elemental analysis which gives an Re/N ratio of 1:1.1. It is likely that the excess rhenium atoms are present as uncoordinated MTO molecules assembled in the MCM channels. This phenomenon may be similar to that reported for MTO encapsulated in zeolite Y,[28] where it was proposed that each supercage contained a cluster of four MTO guest molecules aggregated by Re=O···Re intermolecular interactions.

Experimental Section

General: All manipulations were carried out using standard Schlenk techniques under nitrogen. Solvents were dried by standard procedures (THF, *n*-hexane and Et_2O with Na/benzophenone ketyl; CH_2Cl_2 with CaH_2), distilled under nitrogen and kept over 4 Å molecular sieves. Lithium diisopropylamide was prepared as described in the literature.[29] 4,4′-Dimethyl-2,2′-bipyridine was purchased from Aldrich and used as received. Microanalyses were performed at the Mikroanalytisches Laboratorium of the Technical University of Munich (M. Barth and co-workers). Powder XRD data were collected with a Phillips X'pert diffractometer using Cu-K_α radiation filtered by Ni. Nitrogen adsorption-desorption measurements were carried out at 77 K, using a gravimetric adsorption apparatus equipped with a CI electronic MK2-M5 microbalance and an Edwards Barocel pressure sensor. Before analysis, pristine calcined MCM-41 was degassed at 723 K overnight to a residual pressure of ca. 10^{-4} mbar. A lower degassing temperature of 413 K was used for the modified materials (to minimize destruction of the functionalities). The specific surface areas (S_{BET}) were determined by the BET method. The total pore volume (V_P) was estimated from the N_2 uptake at $p/p_0 \approx 0.95$, using the liquid nitrogen density of 0.8081 g cm^{-3}. The pore size distribution curves (PSD, the differential volume adsorbed with respect to the differential pore size per unit mass as a function of pore width) were computed from the desorption branch of the experimental isotherms, using a method based on the area of the pore walls.[18,30] Assuming open cylindrical pores of radius r_p, zero contact angle, and accounting for the statistical film thickness (t), r_p is given by the sum of the Kelvin radius and t.[18] The t values were derived from a standard nitrogen isotherm for nonporous hydroxylated silica (available from the literature[31]) using the Halsey equation.[18] Although it is known that such traditional methods based on the Kelvin equation underestimate the pore sizes in the range up to ca. 7.5 nm,[32] in this work these calculations are only intended to monitor changes in pore sizes after complexation, by comparing with the parent MCM-41. TGA studies were performed using a Perkin−Elmer TGA7 thermobalance system at a heating rate of 10 K min^{-1} under

nitrogen. IR spectra were measured with a Unican Mattson Mod 7000 FTIR spectrometer using KBr pellets. Raman spectra were recorded with a Bruker RFS 100/S FT Raman spectrometer using a 1064 nm excitation wavelength of the Nd/YAG laser. ^{1}H and ^{13}C solution NMR spectra were obtained with a Bruker AMX-300 spectrometer. ^{29}Si and ^{13}C solid-state NMR spectra were recorded at 79.49 and 100.62 MHz, respectively, with a (9.4 T) Bruker Avance 400P spectrometer. ^{29}Si MAS NMR spectra were recorded with 40° pulses, spinning rates 5.0−5.5 kHz and 60 s recycle delays. ^{29}Si CP MAS NMR spectra were recorded with 5.5 μs ^{1}H 90° pulses, 8 ms contact time, a spinning rate of 4.5 kHz, and 4 s recycle delays. ^{13}C CP MAS NMR spectra were recorded with a 4.5 μs ^{1}H 90° pulse, 2 ms contact time, a spinning rate of 8 kHz, and 4 s recycle delays. Chemical shifts are quoted in parts per million from tetramethylsilane (TMS). Re L_I- and L_{III}-edge X-ray absorption spectra were measured at 20 K in transmission mode on beamline BM29 at the ESRF (Grenoble), operating at 6 GeV in 2/3 filling mode with typical currents of 180−190 mA. One scan was performed for each sample and set up to record the pre-edge at 5 eV steps and the post-edge region in 0.025−0.05 Å^{-1} steps, giving a total acquisition time of ca. 40 min per scan. The order-sorting double Si(311) crystal monochromator was detuned to give 50% harmonic rejection. Solid samples were diluted with BN and pressed into 13 mm pellets. Air-sensitive samples were handled under an inert gas. Ionization chamber detectors were filled with Ar to give 30% absorbing I_o (incidence) and 70% absorbing I_t (transmission). The programs EXCALIB and EXBACK (SRS Daresbury Laboratory, UK) were used in the usual manner for calibration and background subtraction of the raw data. XAFS curve-fitting analyses, by least-squares refinement of the non-Fourier-filtered k^3-weighted XAFS data, were carried out using the program EXCURVE (version EXCURV98[33]) using fast curved-wave theory.[34] Theoretical phase shifts were obtained within this program using ab initio calculations based on the Hedin Lundqvist/von Barth scheme.

4-(*n*-Butyl)-4′-methyl-2,2′-bipyridine: Prepared by modification of a literature procedure.[29] A solution of 4,4′-dimethyl-2,2′-bipyridine (0.50 g, 2.71 mmol) in THF (15 mL) was added to a THF solution of lithium diisopropylamide (2.71 mmol). After 2 h, the orange-brown solution was cooled to −20 °C and $CH_3CH_2CH_2Br$ (0.25 mL) added. After 2 h, iced water was added to the green reaction mixture. The organic solution was dried with Na_2SO_4 and the solvent removed to give the crude product. The yellow residue was purified by recrystallization from diethyl ether to give a colorless solid. Yield: 0.55 g, 89%. $C_{15}H_{18}N_2$ (226.32): calcd. C 79.61, H 8.02, N 12.38; found C 79.48, H 7.98, N 12.18. IR (KBr): $\tilde{\nu}$ = 2957 m, 2925 s, 2870 m, 1596 s, 1553 m, 1460 s, 1376 m, 1104 m, 1023 m, 992 m, 824 s, 799 m, 670 m, 515 m cm^{-1}. Raman: $\tilde{\nu}$ = 3054 s, 2920 s, 2873 sh, 1607 s, 1561 s, 1487 w, 1442 m, 1379 w, 1315 m, 1290 m, 1237 m, 1159 w, 1110 w, 997 s, 737 m, 525 m, 344 w, 237 m cm^{-1}. ^{1}H NMR ($CDCl_3$, room temp., 300 MHz, TMS): δ = 0.86 (t, 3 H, CH_3), 1.29 (m, 2 H, CH_2), 1.60 (m, 2 H, CH_2), 2.36 (s, 3 H, py-CH_3), 2.62 (t, 2 H, py-CH_2), 7.05 (d, 2 H, py-H), 8.15 (s, 2 H, py-H), 8.47 (t, 2 H, py-H). ^{13}C {^{1}H} NMR ($CDCl_3$, room temp., 75.47 MHz, TMS): δ = 13.9 (CH_3CH_2), 21.2 (py-CH_3), 22.4 (CH_3CH_2), 32.5 (py-CH_2CH_2), 35.2 (py-CH_2), 121.3, 122.0, 123.9, 124.6, 148.9, 152.9, 156.0 (all py-C).

MCM-41 Functionalized with 4-[(−CH_2)$_4$]-4′-CH_3-2,2′-bipyridine (MCM-41-bpy): Prepared as described previously.[15] Raman: $\tilde{\nu}$ = 3057 m, 2899 s, 1607 s, 1559 s, 1440 s, 1314 s, 997 s, 732 w, 650 w, 238 m cm^{-1}.

MCM-41 Functionalized with Methyltrioxorhenium(VII) (MCM-41-bpy/MTO): To a suspension of MCM-41-bpy (0.50 g) in CH_2Cl_2 (5 mL) a solution of MTO (0.23 g, 0.92 mmol) in CH_2Cl_2 (10 mL) was added and the mixture stirred at room temperature for 24 h. The solution was filtered off and the pale yellow powder washed repeatedly with CH_2Cl_2 (4 × 20 mL), before drying under vacuum at room temperature for several hours; found C 11.80, H 2.40, Cl 3.34, N 0.83, Re 10.24, Si 27.70. IR (KBr): $\tilde{\nu}$ = 2938 w, 1559 w, 1438 w, 1384 w, 1233 sh, 1067 vs, 961 s, 921 vs, 913 vs, 801 s, 550 sh, 465 vs cm^{-1}. Raman: $\tilde{\nu}$ = 3069 w, 2913 m, 1611 m, 1556 m, 1484 w, 1442 w, 1317 m, 1031 m, 997 m, 941 m, 918 w, 733 w, 474 w, 237 w cm^{-1}. ^{29}Si MAS NMR: δ = −109.8, −102.0 (sh), −66.6, −58.5. ^{29}Si CP MAS NMR: δ = −109.8 (Q^4), −101.7 (Q^3), −66.7 (T^3), −58.7 (T^2). ^{13}C CP MAS NMR: δ = 9.6 [(−O)$_3$SiCH$_2$−], 21.8 (py-CH_3), 26.0 [(−O)$_3$SiCH$_2$*C*H$_2$− and Re−CH_3], 35.0 (py−CH_2CH_2−), 46.1 [Si(O*Me*)$_n$$CH_2$R and −$CH_2$Cl], 125.7, 149.3, 155.0 (all py-C).

(4,4′-Dimethyl-2,2′-bipyridine)(methyl)trioxorhenium (2): Prepared as described previously.[10b] Raman: $\tilde{\nu}$ = 3067 m, 2921 m, 1614 s, 1556 s, 1489 m, 1418 m, 1376 w, 1319 s, 1176 m, 1029 s, 937 vs, 912 s, 846 m, 833 m, 742 m, 668 w, 555 m, 474 s, 355 m, 343 m, 316 w, 271 m, 243 m, 196 m, 157 m cm^{-1}. ^{13}C CP MAS NMR: δ = 20.8 (py-CH_3), 22.8, 27.3 (Re−CH_3), 122.5, 126.8, 145.0, 149.4, 153.2, 154.7 (all py-C).

[4-(*n*-Butyl)-4′-methyl-2,2′-bipyridine](methyl)trioxorhenium (3): To a solution of MTO (0.56 g, 2.25 mmol) in CH_2Cl_2 (5 mL) 1 equiv. of 4-(*n*-butyl)-4′-methyl-2,2′-bipyridine was added. The resulting yellow solution was stirred for 1 h at room temperature. The solvent was evaporated, and the product washed with hexane and dried under vacuum. Yield: 1.02 g, 95%. $C_{16}H_{21}N_2O_3Re$ (475.56): calcd. C 40.41, H 4.45, N 5.89; found C 40.36, H 4.41, N 5.73. IR (KBr): $\tilde{\nu}$ = 3122 m, 3065 m, 3030 m, 2953 s, 2923 s, 2860 m, 1615 vs, 1555 s, 1492 s, 1466 m, 1419 s, 1375 m, 1310 s, 1243 m, 1030 s, 940 vs (Re=O), 918 vs (Re=O), 848 vs, 831 vs, 737 s, 555 m (Re−C), 540 m, 524 m, 480 m, 424 m, 358 s cm^{-1}. Raman: $\tilde{\nu}$ = 3070 m, 2921 s, 1615 s, 1555 s, 1495m, 1423 m, 1325 s, 1171 m, 1030 s, 937 vs, 916 m, 848 m, 743 m, 667 w, 555 w, 481 s, 352 m, 316 w, 265 m, 195 m cm^{-1}. ^{1}H NMR ($CDCl_3$, room temp., 300 MHz, TMS): δ = 0.98 (t, 3 H, CH_3), 1.09 (s, 3 H, Re−CH_3), 1.43 (m, 2 H, CH_2), 1.72 (m, 2 H, CH_2), 2.58 (s, 3 H, py-CH_3), 2.81 (t, 2 H, py-CH_2), 7.38 (d, 2 H, py-H), 8.09 (d, 2 H, py-H), 8.92 (m, 2 H, py-H). ^{13}C {^{1}H} NMR ($CDCl_3$, room temp., 75.47 MHz, TMS): δ = 13.8 (CH_3CH_2), 21.6 (py-CH_3), 22.3 (CH_3CH_2), 27.0 (Re−CH_3), 32.3 (py-CH_2CH_2), 35.4 (py-CH_2), 123.1, 123.8, 126.5, 127.2, 148.9, 150.2, 151.9, 156.7 (all py-C). ^{13}C CP MAS NMR: δ = 13.8 (CH_3CH_2), 21.1 (py-CH_3), 24.4 (CH_3CH_2), 27.4 (Re-CH_3), 33.5 (py-CH_2CH_2), 36.3 (py-CH_2), 125.2, 127.9, 128.7, 146.9, 148.0, 150.3, 153.3, 158.1 (all py-C).

Acknowledgments

This work was partly funded by FCT, POCTI and FEDER (Project PCTI/1999/QUI/32889). Financial support was also obtained from the Alexander von Humboldt foundation (to P. F.), Bayerische Forschungsstiftung (to I. S. G.), Deutsche Forschungsgemeinschaft and Fonds der Chemischen Industrie. A. A. V and M. P. thank FCT for post-doctoral grants, and C. N. thanks the University of Aveiro for a research grant. F. E. K. additionally thanks Prof. Dr. W. A. Herrmann for continuous and generous support. We are grateful to the director of the ESRF for the provision of facilities and to Stuart Ansell (local contact on BM29) for help in the XAFS

experiments. We also wish to thank Pedro Vaz for help with the Raman experiments and Marta Lopes for recording MAS spectra.

[1] [1a] G. S. Owens, J. Arias, M. M. Abu-Omar, *Catal. Today* **2000**, *55*, 317−363. [1b] F. E. Kühn, A. M. Santos, I. S. Gonçalves, C. C. Romão, A. D. Lopes, *Appl. Organomet. Chem.* **2001**, *15*, 43−50. [1c] F. E. Kühn, W. A. Herrmann, *Chemtracts: Org. Chem.* **2001**, *14*, 59. [1d] W. Adam, C. M. Mitchell, C. R. Saha-Möller, O. Weichold, *Struct. Bonding* **2000**, *97*, 237−286. [1e] J. H. Espenson, *Chem. Commun.* **1999**, 479−488. [1f] C. C. Romão, F. E. Kühn, W. A. Herrmann, *Chem. Rev.* **1997**, *97*, 3197−3246.

[2] [2a] W. A. Herrmann, R. W. Fischer, D. W. Marz, *Angew. Chem. Int. Ed. Engl.* **1991**, *30*, 1638−1641. [2b] W. A. Herrmann, R. W. Fischer, W. Scherer, M. U. Rauch, *Angew. Chem. Int. Ed. Engl.* **1993**, *32*, 1157−1160.

[3] [3a] W. A. Herrmann, J. P. Zoller, R. W. Fischer, *J. Organomet. Chem.* **1999**, *579*, 404−407. [3b] T. H. Zauche, J. H. Espenson, *Inorg. Chem.* **1998**, *37*, 6827−6831.

[4] W. Adam, W. A. Herrmann, J. Lin, C. R. Saha-Möller, R. W. Fischer, J. D. G. Correia, *Angew. Chem. Int. Ed. Engl.* **1994**, *33*, 2475−2476.

[5] [5a] W. R. Thiel, R. W. Fischer, W. A. Herrmann, *J. Organomet. Chem.* **1993**, *459*, C9−C11. [5b] W. A. Herrmann, J. D. G. Correia, F. E. Kühn, G. R. J. Artus, C. C. Romão, *Chem. Eur. J.* **1996**, *2*, 168−173.

[6] W. A. Herrmann, R. W. Fischer, M. U. Rauch, W. Scherer, *J. Mol. Catal.* **1994**, *86*, 243−266.

[7] [7a] J. Rudolph, K. L. Reddy, J. P. Chiang, K. B. Sharpless, *J. Am. Chem. Soc.* **1997**, *119*, 6189−6190. [7b] W. A. Herrmann, F. E. Kühn, M. R. Mattner, G. R. J. Artus, M. R. Geisberger, J. D. G. Correia, *J. Organomet. Chem.* **1997**, *538*, 203−209.

[8] W. A. Herrmann, R. M. Kratzer, H. Ding, W. R. Thiel, H. Glas, *J. Organomet. Chem.* **1998**, *555*, 293−295.

[9] [9a] C. Copéret, H. Adolfsson, K. B. Sharpless, *Chem. Commun.* **1997**, 1565−1566. [9b] H. Adolfsson, A. Converso, K. B. Sharpless, *Tetrahedron Lett.* **1999**, *40*, 3991−3994. [9c] H. Adolfsson, C. Copéret, J. P. Chiang, A. K. Yudin, *J. Org. Chem.* **2000**, *65*, 8651−8658.

[10] [10a] F. E. Kühn, A. M. Santos, P. W. Roesky, E. Herdtweck, W. Scherer, P. Gisdakis, I. V. Yudanov, C. D. Valentin, N. Rösch, *Chem. Eur. J.* **1999**, *5*, 3603−3615. [10b] P. Ferreira, W. -M. Xue, É. Bencze, E. Herdtweck, F. E. Kühn, *Inorg. Chem.* **2001**, *40*, 5834−5841.

[11] [11a] W. Adam, C. M. Mitchell, *Angew. Chem. Int. Ed. Engl.* **1996**, *35*, 533−534. [11b] W. Adam, C. M. Mitchell, C. R. Saha-Möller, O. Weichold, *J. Am. Chem. Soc.* **1999**, *121*, 2097−2103.

[12] W. Adam, C. R. Saha-Möller, O. Weichold, *J. Org. Chem.* **2000**, *65*, 2897−2899.

[13] R. Neumann, T. -J. Wang, *Chem. Commun.* **1997**, 1915−1916.

[14] K. Dallmann, R. Buffon, *Catal. Commun.* **2000**, *1*, 9−13.

[15] C. Nunes, A. A. Valente, M. Pillinger, A. C. Fernandes, C. C. Romão, J. Rocha, I. S. Gonçalves, *J. Mater. Chem.*, accepted for publication.

[16] [16a] B. Marler, U. Oberhagemann, S. Vortmann, H. Gies, *Micropor. Mater.* **1996**, *6*, 375−383. [16b] W. Hammond, E. Prouzet, S. D. Mahanti, T. J. Pinnavaia, *Micropor. Mesopor. Mater.* **1999**, *27*, 19−25.

[17] P. Ferreira, I. S. Gonçalves, F. E. Kühn, M. Pillinger, J. Rocha, A. Thursfield, W. M. Xue, G. Zhang, *J. Mater. Chem.* **2000**, *10*, 1395−1401.

[18] S. J. Gregg, K. S. W. Sing, *Adsorption, Surface Area and Porosity*, 2nd ed., Academic Press, London, **1982**.

[19] W. A. Herrmann, W. M. Wachter, F. E. Kühn, R. W. Fischer, *J. Organomet. Chem.* **1998**, *553*, 443−452.

[20] J. Mink, G. Keresztury, A. Stirling, W. A. Herrmann, *Spectrochim. Acta A* **1994**, *50*, 2039−2058.

[21] A. M. Santos, F. E. Kühn, W.-M. Xue, E. Herdtweck, *J. Chem. Soc., Dalton Trans.* **2000**, 3570−3574.

[22] S. Köstlmeier, G. Pacchioni, W. A. Herrmann, N. Rösch, *J. Organomet. Chem.* **1996**, *514*, 111−117.

[23] M. Fröba, K. Lochte, W. Metz, *J. Phys. Chem. Solids* **1996**, *57*, 635−641.

[24] M. Fröba, O. Muth, *Adv. Mater.* **1999**, *11*, 564−567.

[25] J. Evans, J. T. Gauntlett, J. F. W. Mosselmans, *Faraday Discuss. Chem. Soc.* **1990**, 107−118.

[26] F. E. Kühn, J. J. Haider, E. Herdtweck, W. A. Herrmann, A. D. Lopes, M. Pillinger, C. C. Romão, *Inorg. Chim. Acta* **1998**, *279*, 44−50.

[27] R. W. Joyner, K. J. Martin, P. Meehan, *J. Phys. C* **1987**, *20*, 4005−4012.

[28] A. Malek, G. Ozin, *Adv. Mater.* **1995**, *7*, 160−163.

[29] D. K. Ellison, R. T. Iwamoto, *Tetrahedron Lett.* **1983**, *24*, 31−32.

[30] J. M. Thomas, W. J. Thomas, *Principles and Practices of Heterogeneous Catalysis*, VCH, Weinheim, **1997**.

[31] M. R. Bhambhani, P. A. Cutting, K. S. W. Sing, D. H. Turk, *J. Colloid Interface Sci.* **1972**, *38*, 109.

[32] C. Lastoskie, K. E. Gubbins, N. Quirke, *J. Phys. Chem.* **1993**, *97*, 4786−4796.

[33] N. Binsted, *EXCURV98*, CCLRC Daresbury Laboratory computer program, **1998**.

[34] [34a] S. J. Gurman, N. Binsted, I. Ross, *J. Phys. C* **1984**, *17*, 143−151. [34b] S. J. Gurman, N. Binsted, I. Ross, *J. Phys. C* **1986**, *19*, 1845−1861.

Received November 8, 2001
[I01444]